Geotechnical Aspects of Underground Construction in Soft Ground, Kastner, Emeriault, Dias, Guilloux (eds)
© 2002 Spécifique, Lyon. ISBN 2-9510416-3-2

Behavior analysis of diaphragm wall in a deep excavation engineering

Hongwei Huang[1], Y. Riou[2], J. Chappaz[2] & Dongmei Zhang[1, 2]
[1]*Tongji University, Shanghai, China*
[2]*Ecole Centrale de Nantes, Nantes, France*

ABSTRACT: Recent years, increasing attention is being given to the movement control in urban area. Though diaphragm wall as a rigid retaining wall has a trend with small movement, various factors cause great movement of ground. This great movement has a distinct conflict with the original preliminary design. To explore more in detail this point a validation work employing a strong finite element code for deformation of diaphragm wall in a deep excavation project in Shanghai was proposed in this paper. The behavior of soil and diaphragm wall, parameters of the modeling was highlighted through our work. Further analysis gives out some useful and interesting quantitative conclusions that will guide engineers in situ to make good decisions.

1 INTRODUCTION

The increasing demand of new infrastructure in urban area has lead to a great number of deep excavations. Due to the limited space, some thin and high rigid retaining walls, such as diaphragm wall with struts, are required. Owing to the possible poor workmanship and scarcely controllable sources, great movement is hard to avoid, and further likely damage the surrounding sensitive structures (Duncan and Bentler 1998, Yoo, 2001). Therefore the excavation has to be controlled, and the modeling of this kind of works requires special care, lot of verification, validation and justification.

The modeling of these retaining walls and their struts has to be justified in order to warrant their stability and respect economic criteria. This is particularly true for the works of large depth in the soft grounds. Generally, there are numerous and reliable traditional methods for calculating this kind of works, for instance, Wong and Broms (1989), Clough and O'Rourke (1990), Hashash and Whittle (1996). However, they come out limited for complex configurations and complicated construction steps. Some researchers using finite element method proved that modeling in a more representative way the behavior of excavation work, its environment and its steps of construction (Addenbrook and Potts, 2000), is possible. Whereas, if this method is sometime used for this type of work, one notice that the engineers have few references to validate modeling using this method and the results.

In order to propose some element of justification to those which are in charge of such calculation or to supply information for a data base of case tests (Riou et.al. 2001), this paper compares some numerical results provided by a finite element code with some measurement on site. The work studied here focus on the behavior of retaining wall in a shaft excavation, which is for launching the pedestrian tunnel under the HuangPu River in Shanghai.

This calculation is posterior to the construction and the measurements on site are known. Thus the goal of this confrontation is to employ a strong finite element code to simulate the behavior of a retaining wall, to highlight the significant parameters of this modeling and to propose procedures likely to represent the behavior of the ground as well as possible.

2 GEOMETRY SHAPE OF EXCAVATION

The geometrical shape of the excavation shaft in Pudong is illustrated in Figures 1and2. The work is 100 m long, 22.8m wide and 22m deep. The retaining wall is diaphragm wall with 37m depth and 0.8m thickness. The bracing system is made up of steel pipes with 609mm in diameter and 11mm in thickness. For the first 15m excavation, the construction sequence includes 5 stages. After each stage, a strut is installed before further excavation. During excavation, some routine measurements were implemented, such as lateral displacement and settlement of wall, earth and pore pressure.

The ground water level is 0.5-1.0m below surface.

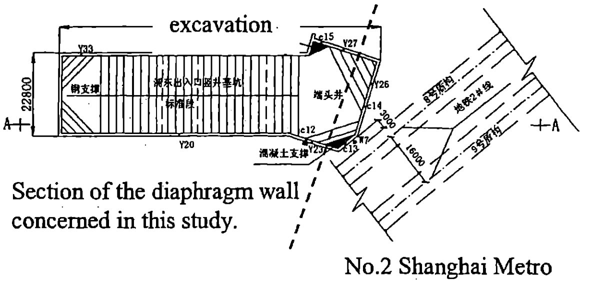

Figure 1. Plan of excavation

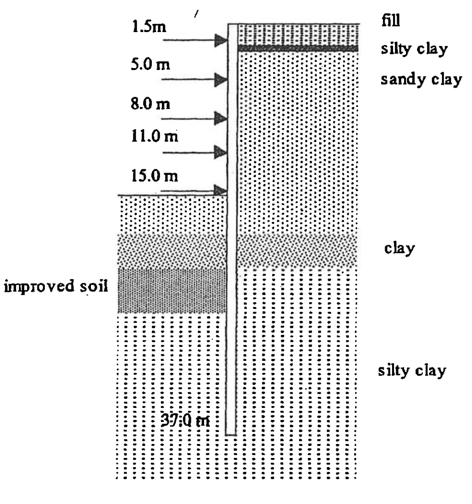

Construction stages up to 15.5 m:

- Improved soil by jet grouting : 20 - 26 m
- Dig to 2 m and the first strut at 1.5m
- Dig to 5.5 m and the second strut at 5.0m
- Dig to 8.5 m and the third strut at 8.0m
- Dig to 11.5 m and the fourth strut at 11.0m
- Dig to 15.5 m and the fifth strut at 15.0m

Figure 2. Vertical section of diaphragm wall

3 MODELLING

The soil is modeled as an elasto-perfectly plastic with a Mohr-Coulomb yield surface and non associated plastic potential defined by an dilation angle. This model has been chosen because of its popular use in projects (Addenbrooke and Potts 2000). The spatial distribution of different layers and their undrained mechanical parameters can be shown in Table 1. These values come from a geotechnical report finished by Shanghai institute of air defense foundation. According to a usual practice (Shanghai foundation design code, 1999), the c and ϕ values were discount 30 % of the peak value from test.

The flexural rigidity EI of wall can be calculated to be 1.19×10^6kN • m^2. The struts are designed as simple bar of two nodes. The equivalent Young's Modulus is calculated as 100000 MPa.

Table 1 Physical and Mechanical Parameters

Layers of soil	γ kN/m^3	c kPa	ϕ °	E MPa	ν	Sup. level m
fill	20	0	10	5	0.3	0
silty clay	18.3	11.3	19.7	4.76	0.3	2
sandy silt	18.3	2.57	31.5	7.52	0.3	2.5
clay	18.1	14.33	15.7	3.95	0.3	20
improved soil	20	15.25	20	60	0.25	22
silty clay2	18.2	15.25	17.2	4.9	0.3	22
silty clay3	20.2	25	23.7	7.74	0.3	42.8
silty sand	19.5	3	35.8	13.86	0.3	46.7

The stiffness of the improved soil zone is obtained by the following expression:

$$E_i = 110 S_u \tag{1}$$

where S_u = the compression strength of cement soil at the 28th day (kPa).

The numerical calculation is performed with the finite element code CESAR, from the Laboratoire Central des Ponts et Chaussées. This code was selected for its facilities making easy the modeling of special current processes in geotechnical works (initial stress, excavation, structure and al.). Due to the shaft geometry, this analysis is a plane strain calculation. The limits of the mesh are at a distance of 100 m from the centerline and 38 m below the base of the wall (no displacement on these limits). The soil and the wall are modeled by 930 eight-node and six-node isoparametric elements (2200 nodes). The struts are simulated as bars. Contact elements are used in the data file dealing with the interface between soil and wall.

The initial stress state is characterized by a geostatic state with a K_0 value of 0.65 (commonly used in Shanghai). The only effect of the construction of the wall is simulated as overweight with 7kN/m^3 in comparison with the unit weight of soil. According to the water table, effective stress method was employed in this calculation.

The calculation takes into account the 5 stages of the construction mentioned previously. Each stage consists of 10 increments. Checking the ratio of absolute global residual force to absolute applied force performs the convergence test. In this analysis, the tolerance is, at least, 0.005.

4 ANALYSIS OF DIFFERENT PATTERNS

4.1 Reference calculation

For this first calculation, no contact element is used, and the mechanics parameters are used from Table 1. Observed and predicted lateral displacements of the wall are shown in Figure 3. The measured records were acquired with the assumption of no displacement at the bottom of the diaphragm wall.

This assumption is not really verified but the survey engineers think this displacement at this point is generally so small that this point is fixed. Figure 3 shows that the calculation has a much bigger movement at the bottom of wall.

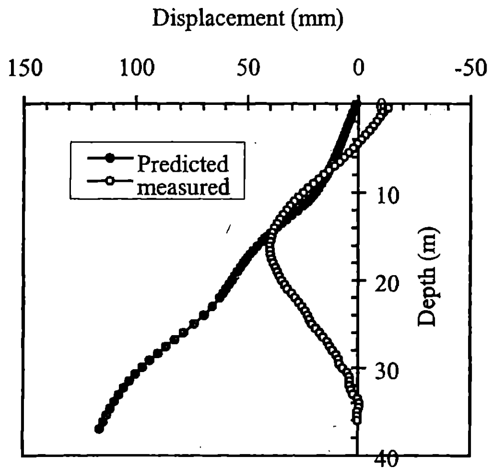

Figure 3. Comparison of measured and predicted lateral displacements

Because of a predicted significant heave of soil in pit and wall, and because of a large lateral displacement at the bottom of the diaphragm wall, these results are considered impossible in practice. So, the calculated results demonstrate the inefficiency of a simple constitutive model and untreated parameters to simulate the behavior of soil.

In Shanghai, some analytical methods are employed to model the excavation engineering. In this kind of method, local unloading is successfully introduced to simulate the real heave of soil in pit. Here this will be adopted into our finite element calculation.

4.2 The first model for a more realistic simulation

In the first model, the effects of localization are artificially implemented by boundary conditions with no horizontal and vertical displacements 8m below the base of the wall. This depth corresponds to 3 times the excavation depth. This artefact is combined with an increase of stiffness in the deep layers. However, there is no recommendation for how the coefficient should be affected to the Young modulus and the position of these layers. The unloading stress path in this zone can justify this increase, different from the stress used in the identification of parameters in geotechnical study. Without information that could lead to a more realistic stiffness, we propose a back analysis for the evaluation of this increasing factor.

4.3 The second model for a more realistic simulation

In a general sense, excavation causes the unloading of soil below excavation surface. And this effect of unloading has a limited depth or zone. Many measurements show that different stages have different depths. Based on the principle of Residual Stress (Liu 1998), this special zone is characterized by a depth Hr and a new stiffness E_u. Below this zone, little disturbance is available, thus it is possible to assume no vertical displacement from the bottom of this zone. A short introduction is outlined below.

From many measured records in Shanghai, the effecting depth of residual stress Hr is evaluated experimentally:

$$Hr = H / (0.0612.H + 0.19) \qquad (2)$$

where H = depth of excavation (m)
Hr = effecting depth of residual stress (m).

The Young's modulus depending on the particular stress path in this zone is calculated by the following expression:

$$E_u = (1 + f(\sigma_1, \sigma_3, K_0, c, \varphi, \sigma_m))^2 \ E_{ui} \qquad (3)$$

$$E_{ui} = \hat{E}_{ui} \ \sigma_m \qquad (4)$$

where E_{ui} = initial unloading modulus
σ_m = mean pressure
$\hat{E}_{ui}$ = coefficient of unloading modulus

Generally, for silty clay under the vertical unloading and horizontal loading stress path, there is a formula below:

$$\hat{E}_{ui} = 1000 / [1.22 (tg^{-1} R)^2 - 3.52(tg^{-1} R) + 8.36] \qquad (5)$$

where R = ratio of loading to unloading.

After using these formulas from (2) to (5), it is likely to obtain the new results through finite element code. Figure 4 shows the comparison of numerical results and measured records.

A good agreement of the predicted lateral displacement using the first model with the observed deflection requires a silty clay Young's modulus three times greater than the original value from laboratory test. This can be clearly understood as the result of unloading stiffness. This factor 3 can be considered as reasonable on the basis of experimental tests. However, it is advisable to confirm this result before a systematic use in the modeling of retaining wall.

Considering the predicted deflection (see Figure 4), one can suppose that the improved soil layer is too stiff and the silty clay below too soft. No more sophisticated back analysis has been carried out considering that we have no formal assurance about a real fixation at the toe of the wall.

The second model gives all information needed for such a modeling, position of the disturbed layer, improved stiffness taking into account a realistic stress path in the zone concerned by the excavation and experimentally justified on field tests. The maximum displacement and its position are in accordance with the observed deflection. Whereas, a distinct disparity occurs between measures and numerical results in the 9 first meters. This is due to the condition of no vertical displacement in the first two stages of calculation. This artefact enables localization of unloading but requires some adaptation for a realistic modeling for the first stage of excavation.

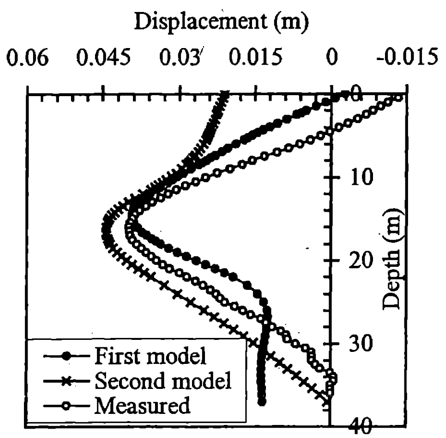

Figure 4. Predicted and observed deflection of the wall: Modified new procedures

Moreover, calculation from the second model presents a consistent heave of soil at each stage with the observation. For instance, the heave of bottom soil at excavation level is about 11cm. That is similar to the general observation for Shanghai soils: 1m excavation causes 1cm heave.

5. ANALYSIS OF SOME KEY PARAMETERS

Owing to its reasonable calculation, the second model was employed to analyze the effects of some key parameters on deformation behavior of wall: soil-wall interface, K_0, struts stiffness and improved soil in pit.

5.1 Effect of contact elements

Figure 5 gives the effect of different contact elements on the lateral displacement of wall. The two curve show that there is much more displacement above the excavation surface. The maximum difference occurs at surface with 33mm for the smooth interface and 21mm for the rough interface. The maximum relative error is 60%. However, due to the resistance action in excavation side below excavation surface, the disparity between two kinds of contact elements decreases gradually from the top of wall to excavation surface. The displacements under the rough elements are closer to measurements than ones under the smooth elements. So, it seems that rough contact is more convenient for the modeling. But, this fact should be further confirmed. This result can depend on the procedure for the second model.

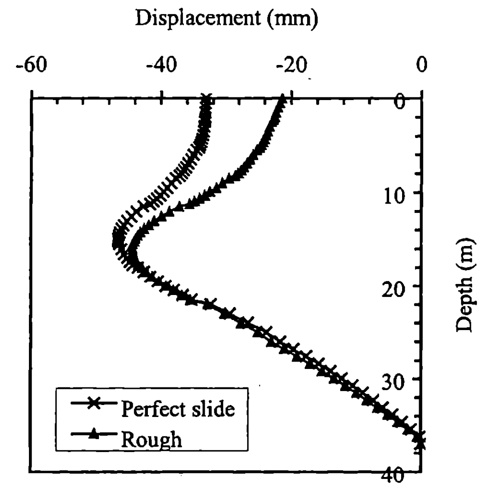

Figure 5. The effect of soil-wall contact on lateral displacement

5.2 Effect of initial K_0

The assessment of K_0 implies special instruments and long geotechnical experience. For this reason, a sensitive study is required in order to evaluate the scatter in predicted deflection. A reasonable variation, in Shanghai, taking into account the soil history and the soil disturbance during the construction clay is: $0.5 < K_0 < 0.9$. Figure 6 illustrates that the wall deflection increases with K_0. From 0.5 to 0.9 of K_0, the lateral displacement increase is 100%.

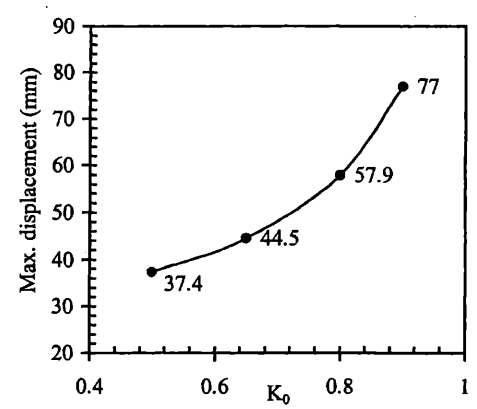

Figure 6. The effect of initial K_0 on lateral displacement

K_0 has two opposite effects on the displacement: larger lateral pressure and restrained plasticity when K_0 increases. This result needs a more elaborate study for a better understanding of this phenomenon.

5.3 Effect of strut stiffness

The curve in Figure 7 shows a significant change in the deflection of the wall due to the change of strut. Here the change of strut is based on the value of EA (E = strut Young's modulus, A = section area). The displacement values indicate the threshold of strut EA should be greater than 4000 MN. Obviously, increasing EA of strut can conduce to cutting down displacement of wall. When the EA increases from 2000MN to 4000MN, the displacement will decrease more than 7.7%, whereas EA increases from 4000 to 6000 and from 6000 to 9000, their corresponding displacement will decrease 2% and 1.8% respectively. It is clear that over-increasing strut should not obtain much benefit to displacement of wall.

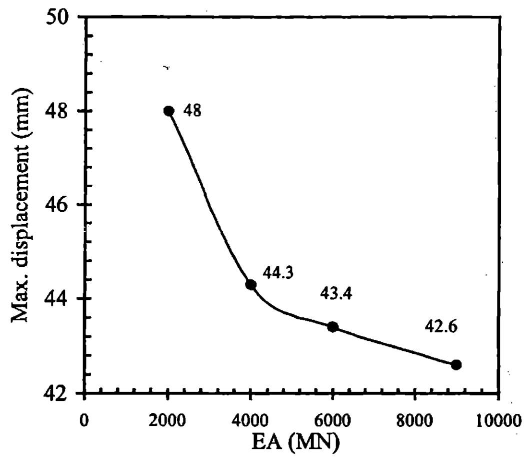

Figure 7. The effect of strut stiffness on lateral displacement

5.4 Effect of improved layer

Many projects show improvement of soil in pit can reduce effectively maximum displacement of wall. However there is a lack of detail values. Here, Table 2 outlines the effect of improved soil on displacement. It can be seen that the maximum displacement decreases 18%, 24% and 32% as the Young's modulus increase by a factor of 4, 6 and 10, respectively. The values proposed here can help engineers to make good decisions when they want to choose higher improvement or great displacement.

Table 2. The effect of improved soil in pit on displacement

E_i (MPa)	10	40	60	100
Maximum displacement (mm)	59	48	44	40

6. DISCUSSIONS AND CONCLUSIONS

Based on previous studies, the aim of this study was to apply FEM calculations to the modeling of a retaining wall in soft Shanghai clay. It was seen that this modeling requires many precautions, especially with very crude models. In order to get some reasonable accordance with the measure, recommendations, generally used for classical methods, need to be implemented. So, except for the top of the wall horizontal displacement, the proposed second model seems to present realistic results. The boundary condition (v=o) is certainly not the best way to simulate the unloading localization but the global behavior of the soil seems correctly modeled. This calculation can be improved by some rearrangements:

- On the excavation side, the use of anisotropic behavior taking into account unloading in vertical direction and loading for the horizontal one due to the compression caused by wall displacement ;
- Behind the wall, the use of an unloading modulus in accordance with the lateral unloading.

Table 3. The effect of parameters on displacement of wall

Parameters	Maximum lateral deformation
Interface: rough→smooth	Increase of 60% for the top of the wall
Soil improvement under the excavation bottom:10→100 Mpa	Decrease of 32%
Strut stiffness: Increase of 300%	Decrease of 8% (for the same spacing)
Initial state: K_0: 0.5→0.9	Increase of 100%

Generally, using FEM calculations, one can hope for an accurate result free from arrangements of parameters in different zones of the engineering works. For that, we need to use some realistic models and especially realistic constitutive relationships. So, we plan to carry on this study by implementing progressively new factors in our modeling. This will be done in order to assess the accuracy of each new implementation. Among these improvements, there are:

- "bilinear elastic" perfectly plastic behavior, with two different Young modulus: one for loading and another one for unloading;
- elasto-plasticity (with hardening): "Cam Clay Modified" model, with linear elasticity and non linear elasticity;
- Coupled modeling;
- Visco-elasto-plasticity;
- 3 D simulation.

However based on second model, the parametric study give out some useful and interesting result about lateral deformation of the wall that will guide engineers to make good decision. The main outcomes are shown on the table 3 as above.

ACKNOWLEDGMENT

This study was supported by the Foundation for University Key Teacher by the Ministry of Education of China and Shanghai Key Discipline Project. We hereby express our great thanks.

REFERENCES

Addenbrooke, T. I., and Potts, D.M.(2000). Displacement flexibility number for multipropped retaining wall design. *J.Geotech. and Geoenvir. Engrg.*, ASCE, 126(8): 969-978.

Clough, G. W., and O'Rourke, T.D.(1990). Construction induced movements of in situ walls. *Proc., Des. and Perf. of Earth Retaining Struct.*, ASCE, New York: 439-470.

Duncan, J.M., and Bentler, D. J.(1998). Evolution of deep excavation technology. *Inter. Confer. On Soil-Structure interaction in Urban Civil Engineering, Darmstadt Geotechnics*, No.4, Vol.1:139-150.

Hashash, Y. M., and Whittle, A. J. (1996). Ground movement prediction for deep excavation in soft clay. *J. Geotech. Engrg.*, ASCE, 122(6):474-486.

Liu, G.B. (1998). The study on unloading deformation of soft clay. *Tongji University Publishing House:* Shanghai.

Riou, Y., Mestat, Ph.. and Humbert P.(2001), Référentiel de tests en géotechnique: une nécessité pour les logiciels. 1ère Conférence Internationale Albert Caquot, Modélisation et Simulation en Génie Civil: Paris

Shanghai Foundation Design Code (DGJ08-11-1999). (1999): Shanghai.

Wong, K. S., and Broms, B. B.(1989). Lateral wall deflections of braced excavation in clay. *J. Geotech. Engrg.*, ASCE, 115(6):853-870.

Yoo, C. S. (2001). Behavior of braced and Anchored walls in Soils Overlying Rock. *J. Geotech. and Geoenvir. Engrg.*, ASCE, 127(3):225-233.